17

Multiscale Manipulations with Multiple Parallel Mechanism Manipulators

Gilgueng Hwang and Hideki Hashimoto
The University of Tokyo
Japan

1. Introduction

While recent years have brought an explosive growth in new microelectromechanical system (MEMS) devices ranging from accelerometers, oscillators, micro optical components, to micro-fluidic and biomedical devices, our concern is now moving towards complex microsystems that combine sensors, actuators, computation and communication in a single micro device. It is widely expected that these devices will lead to dramatic developments and a huge market, analogous to microelectronics.

However, several problems (e.g., sticking effect) exist which are preventing fully autonomous manipulation with dextrous skills at the micro-scale. Dextrous manipulation, requiring precise control of forces and motions, cannot be accomplished with a conventional robotic gripper; any slave should be more anthropomorphic in design. These kinds of dextrous manipulations still need human operator assistance.

Task-based autonomous manipulation has been explored by many researchers to overcome micromanipulation problems. Fearing et al. developed an automated microassembly system with ortho-tweezers and force sensing (Fearing et al., 2001). However, the workspace was really small and the range of the target object was pretty much limited.

Inspection, prototyping or repairing of a miniaturized system which require human's flexible intelligence relies on the human's operation under a microscope. These tasks are very stressful and cannot be done by an autonomous system such as Fearing's prototyping machine. As a human-centred manipulation, teleoperation has been researched for the ability to display the expanded micro environment to the human operator. By combining with haptic interfaces which provide force feedback, a human operator could operate a micro scale object with enough telepresence and reality, increasing the human's operability and operational efficiency. There are many applications based on bilateral teleoperation control (Kosuge et al., 1995; Hannaford & Anderson, 1988). A chopstick-like micromanipulation system having a two-fingered micro-hand as a slave was developed (Tanikawa & Arai, 1999). However, this system did not support force feedback to the operator, which does not provide enough telepresence. A surgical system such as the da Vinci System (Dosis et al., 2003) is a good application since humans and robots collaborate with each other for the purpose of high performance with safety. In our previous work, a tele-micromanipulation system was proposed to enable micro tasks without stress (Ando et

Source: Parallel Manipulators, New Developments, Book edited by: Jee-Hwan Ryu, ISBN 978-3-902613-20-2, pp. 498, April 2008, I-Tech Education and Publishing, Vienna, Austria

al., 2001). The above teleoperated systems had enough functionality in a specified application target instead of losing dexterity during operation.

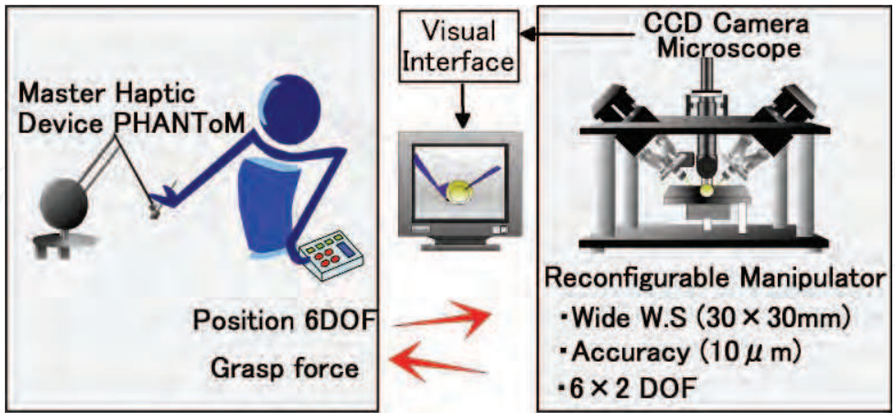

Fig. 1. Concept of micromanipulation system using multiple parallel mechanism micromanipulators

There are still many applications which require human intelligence to overcome the limitation of artificial intelligence (AI) technology and the limited dexterity of the slave manipulator. For these reasons, humans should intervene in the manipulation process. Dexterous manipulation, requiring precise control of forces and motions, cannot be accomplished with a conventional robotic gripper; a slave should be more anthropomorphic in design. These kinds of dextrous manipulations still need a human operator's assistance. In the mean while, the single-master multi-slave (SMMS) system was developed using the virtual internal model (Kosuge et al., 1990). It enables better dexterous teleoperation system without increasing the human's operational d.o.f. However, their work relied on the reference position distribution without considering the force feedback which made the comparative analysis with other systems. The communication delay issue of SMMS teleoperation by decomposing the dynamics of multiple slaves has been studied showing several simulated results (Lee & Spong, 2005). However, it was not implemented to the real time system for the practical systems different dynamics than the theory.

These concepts of multiple robot configurations from macro scale can be the break through of conventional micro/nanomanipulation.In our research, we implement dexterous micromanipulation system based on the SMMS concept (Hwang et al., 2007). A single PHANToM haptic device as a master device and dual 6-d.o.f. parallel micromanipulators as slave devices are adopted as shown in Fig. 1.

Using dual-slave manipulators is expected to enhance the performance or dexterity of the total system compared to our previous work, which had a single slave manipulator (Ando et al., 2001).

This chapter continues with the system structure of tele-micromanipulation systems and the parallel manipulator as a slave device is briefly introduced. The singular position and manipulability analyses are done in the Section 3. Section 4 covers the overall strategy and the mapping method between the PHANToM master device and the dual slave manipulators. Finally, several experimental results (e.g., accuracy evaluation, master–slave position/force-mapping method) are shown. Notation is based on the reference (Paul, 1981).

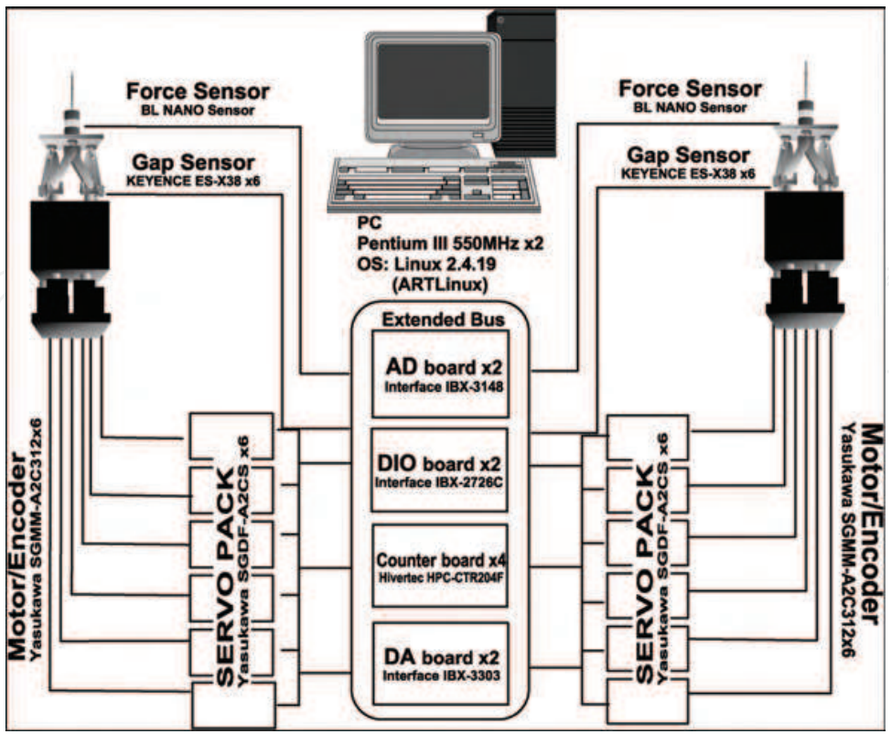

Fig. 2. Electronics and control box for dual parallel mechanism micromanipulators connected to the pc

2. SMMS system overview

In this section, a tele-micromanipulation system is introduced. Figure 2 shows the configuration of our tele-micromanipulation system. A parallel manipulator having an

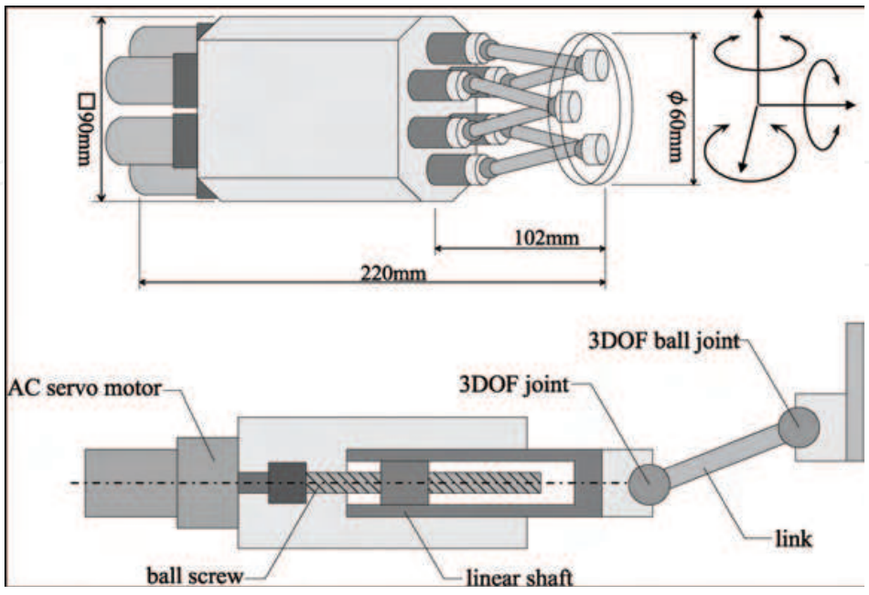

Fig. 3. Parallel mechanism micromanipulator

original mechanism is used as a slave manipulator in the teleoperation system. The slave manipulator and master system are connected using an Ethernet and they are used to perform teleoperations through the network. A bilateral control system was adopted to realize the overall teleoperation system.

2.1 SMMS architecture

The proposed SMMS tele-micromanipulation system is an extension of our previous system (Ando et al., 2001) that supported 1:1 master–slave tele-micromanipulation.
We proposed a prototype of the SMMS tele-micromanipulation system which applies dual-parallel micromanipulators in a 'V' configuration which is similar to the natural human hand position while assembling or manipulating an object.
Figure 1 show the overall system configuration including the master haptic device, slave manipulators and the visual interface connected on RT-Middleware (Ando et al., 2005). RT-Middleware technology has several advantages for constructing SMMS system architecture such as providing a flexible network connection environment which is required for multi-modal displaying or human–robot shared control. The shared controller plays a major role in generating the multi-slave's reference position and internal force by human–robot cooperation. However, in this paper, we do not go further with the shared control. Each slave controller drives six link shafts to position the parallel mechanism end-effector within about 10 μm positioning accuracy. There are three RT components with a position/force IO interface through the network. Both slave manipulators are controlled by a PC (Pentium III 500 MHz × 2). A real-time extension for Linux (ART-Linux) is used as the operating system to perform motion control at 1-kHz sampling rate.
The slave manipulator with a parallel link mechanism as shown in Fig. 3 is used as a slave manipulator. Compared to the serial mechanisms used in normal robot arms, the parallel mechanism has merits such as high stiffness, high speed and high precision.
A serial link mechanism PHANToM haptic device is adopted as our master device. This device allows the 6-d.o.f. measurement including 3 d.o.f. of each translational and rotational motion. Also, the 3-d.o.f. translational force feedback is supported by this master device. Real Time Linux was used as the operating system to control the master with 1-kHz sampling frequency.

3. Kinematics analysis of slave device

It has already been mentioned in Section 2 that there exist several characteristics of a novel parallel mechanism slave micromanipulator being used in this research. However, in the cooperative manipulation of a multi-slave system, several problems of parallel manipulators such as a singular position possibly become more serious than in independent manipulation. Therefore, singular position and the manipulability of the parallel manipulator used in this research are discussed in this section.
The most feasible arrangement of both manipulators considering the result of manipulability is also described in the latter part in this section.

3.1 Inverse kinematics of parallel micromanipulator

It is already mentioned in chapter.3 that there exist several characteristics of a novel parallel mechanism slave micromanipulator being used in this research. However, in the

cooperative manipulation of multi-slave system, several problems of parallel manipulators such as singular position possibly become more serious than in the independent manipulation. Therefore, analyses on the kinematics, singular position, and manipulability of the parallel manipulator which is used in this research should be given in this section. The most feasible arrangement of both manipulators is also described in the latter part in this section. An inverse kinematics analysis on the parallel mechanism micromanipulator is described in this section. Figure 4 shows coordinate system adopted for kinematics analysis. Point O is the origin and the criteria coordinate is the base coordinate system.

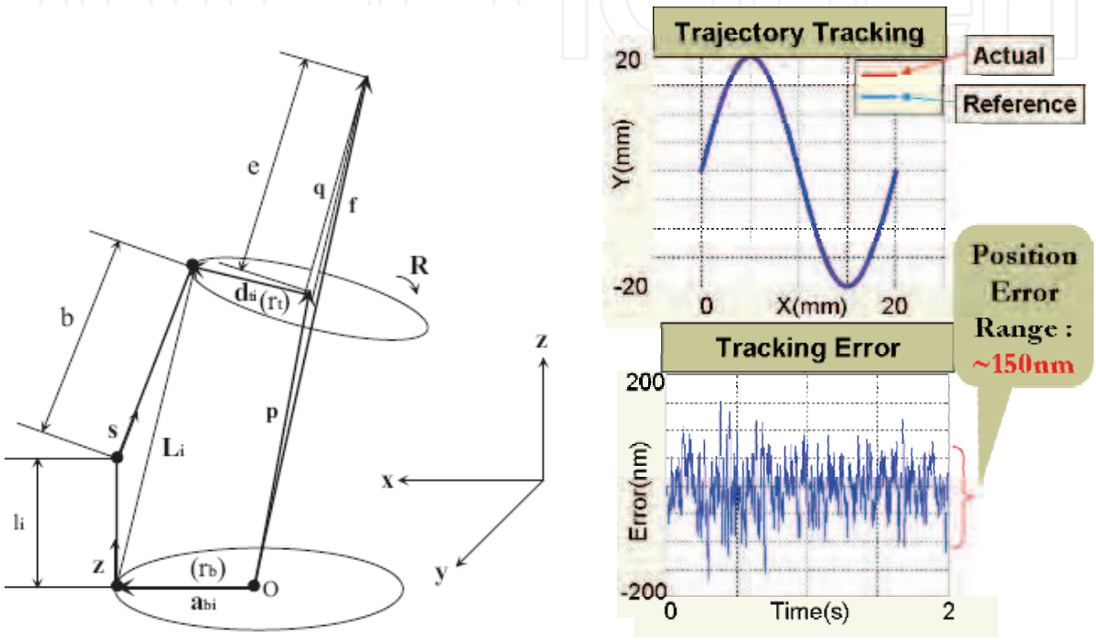

(a) (b)

Fig. 4. Coordinate system of parallel mechanism manipulator (a), and position tracking (b)

We define each variables and constants in the following manner.

(ϕ, θ, φ) : posture of end-effector,

R : Rotation matrix which represents the posture of the end-effector,

i : Chain number,

a_b : Vector from centre of base to base joints,

r_b : Length of a_b ,

d_t : Vector from centre of end-plate to end-table joints,

r_t : Length of d_t ,

z : Unit vector from base joint datum point to actuator joints datum point,

l_i : Length of chain of prismatic joints,

s : Unit vector from actuator joints datum point to end-plate joints datum point,

From relations between base joints and end-effector joints, we get

$$p + Rd_{ti} - a_{bi} = l_i z + bs, \tag{1}$$

Where L_i is used for $p + Rd_{ti} - a_{bi}$.

$$L_i - l_i z = bs\,. \tag{2}$$

Both sides of equation are squared and because $z^2 = 1, s^2 = 1,$ and we get the following equation.

$$l_i^2 - 2(L_i \cdot z)l_i + L_i^2 - b^2 = 0. \tag{3}$$

This equation is solved for l_i, and we get,

$$l_i = (L_i \cdot z) \pm \sqrt{b^2 - L_i^2 + (L_i \cdot z)^2}\,. \tag{4}$$

Where, $L_i = (L_x, L_y, L_z), z = (0,0,1)$ and using the constraints that the chains sign of square root is negative, we get the following equation.

$$l_i = L_{zi} - \sqrt{b^2 - L_{xi}^2 - L_{yi}^2}\,. \tag{5}$$

Thus, the length of the link l_i is determined by the tip position of the end-effector $F(x, y, z, \varphi, \theta, \phi)$. In other words, we can compute the reference link length l_{1-6} from the position and posture of end-effector.

A simulation was conducted to verify the validity of the calculated inverse kinematics for our purpose. As y-directional reference sinusoidal input for simulation is set as following.

$$Y = 20 \sin 2\pi t \tag{6}$$

The resolution of encoder attached to each linear driving link is given as the 0.122μm. Figure 4b shows the result of the simulation. It is quite well being tracked to the given sinusoidal trajectory with the maximum tracking error 0.150μm. This result proves the validity of the inverse kinematics calculation conducted here, also almost of the error is generated from the quantization process with the encoder resolution.

3.1 Singular position analysis

There exists a singular position in the manipulator workspace. The d.o.f., decreases around this position or point. Therefore, it should be avoided in the control of the manipulator. Here, we need to analyze this singular position of our system by some calculations.

First of all, the Jacobian matrix can be mathematically defined as follows. Assuming that an n-d.o.f. manipulator is working in an m-dimensional task space, where $m < n$, we have:

$$v = J_v(x)i \tag{7}$$

Where v and i indicate the Cartesian and joint velocity vectors defined in the task space R^n and the joint space R^m, respectively, and J_v represents a $m \times n$ Jacobian matrix. J_v is also considered as a Jacobian matrix which contains ϕ as an Euler angle.

In the case that we put the column vector of J_v as M_j (j = 1 ~ 6), the relation between v and i can be described as:

$$v = \sum_{j=1}^{6} i_j M_j \,, \tag{8}$$

Therefore, the singular position can be obtained by the calculation of the determinant of the Jacobian matrix J_v :

$$\det J_v = 0 \tag{9}$$

The singular position may cause some problems which can be measured by the manipulability. Therefore, we need to visualize the manipulability of dual manipulators on the overall workspace.

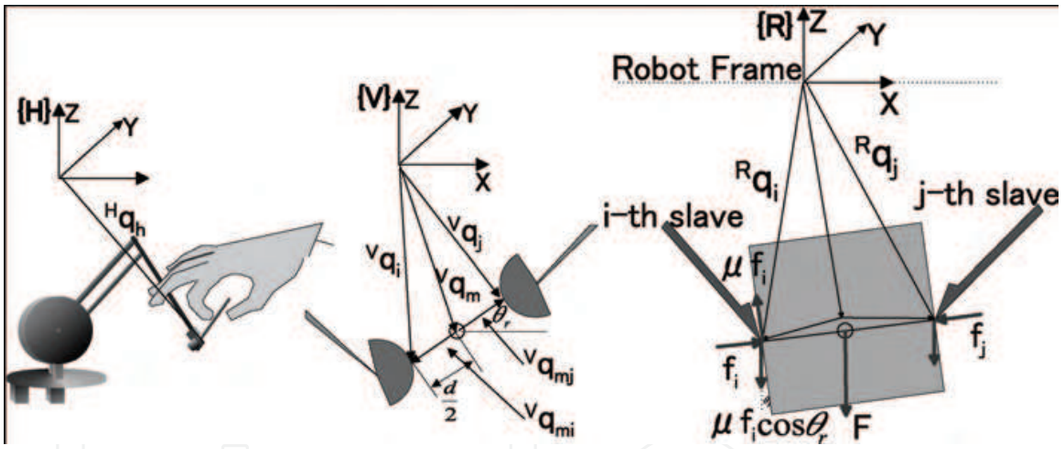

Fig. 5. Kinematical model of the cooperative system. The universe, and left and right manipulator's coordinate frames are described as {A}, {B}, {C}, respectively.

3.2 Multi-micromanipulator analysis

In the case of the dual-micromanipulator system, a proper coordinate system for each manipulator needs to be analyzed. Figure 5 shows the proposed model of the cooperative system.

There are several advantages of this design which can be summarized as high flexibility to random target objects, high dexterity, etc.

The angle between two manipulators is 90◦ and the initial points of the end-effector are set as (5, 0, 5) mm and (−5, 0, 5) mm. Frame B is described by:

$$^{A}_{B}C = Rot(y,45) \cdot Trans(5,0,-5), \tag{10}$$

$$ {}^{A}_{C}C = Rot(y,-45)\cdot Trans(-5,0,-5). \tag{11} $$

Equations (10) and (11) show the conversion matrix for arranging the coordinate system of each manipulator.

3.3 Manipulability measure

The manipulability measure w is proposed to measure quantitatively the ability to change the position and orientation of the end-effector from the view point of the kinematics (Yoshikawa, 1985). There is also a trade-off between accuracy and manipulability. As the proposed parallel manipulator has no redundant d.o.f., w is represented as follows:

$$ w = \left|\det(J_v)\right|. \tag{12} $$

The kinematical manipulability in the dual-micromanipulator's workspace which is parallel to the xy plane can be referred from the reference (Hwang et al., 2007). The human operator is possibly able to avoid the singular position which is located around the position with zero manipulability. It is easily verified that mapping the centre position of both manipulators with the haptic reference position gives consistency of manipulability, because manipulability is plotted as symmetrical to the plane x = 0.

4. Manipulation strategy

4.1 Master/slave mapping

Figure 5 depicts the kinematical model of the proposed system including mapping method. The reference position of the haptic device is mapped into the centric of both end-effectors' tip positions. At the same time, the internal force generated by both end-effectors conflicts with the target object is fed into the user through the haptic device. In this section, a novel mapping method between the SMMS system arranged as shown in sections 2 and 3 and finally a valid manipulation strategy are discussed. Basically, the reference position of the haptic device should be scaled into the center of both manipulators' tip positions during the free motion. The reference position to each slave manipulator is calculated from the current position and posture of the haptic device. It enables to assure more workspace for both of manipulators. Also, the same manipulability of both manipulators can be obtained on z axis (xy=0), because the manipulability of both manipulators is symmetrically plotted to the plane x = 0. It can be the most feasible interface to the human operator with only two-dimensional visual information. Several experimental results to verify the proposed mapping method will further be shown in section 5.

4.2 Virtual mapping method

This section introduces a novel mapping method between SMMS devices arranged as shown in the section 2 and 3 (see Figure 1) and an improved manipulation strategy is proposed in order to emphasize the human manipulation in the micro world.

Since the master device and the slave devices have very different kinematical structures in this system, the usual direct mapping method (e.g., joint-to-joint mapping) cannot be useful in our system. A virtual mapping method was used to connect between the human's hand and the non-anthrophormous slave device, where their feedback strategy was based on the fingertip-level force feedback (Griffin et al., 2003). Our system has the serial link master device but the parallel link slave devices that define a new manipulation approach. This

paper introduces a novel approach to realize more dexterous control with the simplified master device to control multiple slave devices, discussed in relation to the object based roll and yaw angle control to adjust the grasp force control. Figure 5 and 6 show this new manipulation approach.

The roll and yaw angle of the phantom haptic interface is measured and used to provide the roll and yaw orientation of the manipulated object. Then the reference grasping force is proportional to the measured pitch angle of PHANToM haptic interface. This reference object size is mapped into the width of both the slave's tip positions.

As shown in Fig. 5, the virtual mapping parameters are described in the virtual robot coordinate which is denoted as V . Given the reference centre position of the virtual object q_m , we need to calculate the reference tip position of each end-effector, q_i, q_j. The centre position of the virtual object is described as ${}^{V}q_m$. ${}^{V}q_{mi}$ and ${}^{V}q_{mj}$ describe the vector from the virtual object centre to each of slave tip position. This term can be obtained from the roll and yaw angles (θ_r, θ_y) commanded from the master haptic device. The reference grasping force F_g^r is generated by the pitch angle (θ_p). Then, ${}^{V}q_{mi}$ and ${}^{V}q_{mj}$ can be calculated by the following rotational matrix:

$$ {}^{V}q_{mi} = \begin{bmatrix} \cos\theta_r \cos\theta_y & -\sin\theta_r & \cos\theta_r \sin\theta_y \\ \sin\theta_r \cos\theta_y & \cos\theta_r & \sin\theta_r \sin\theta_y \\ -\sin\theta_y & 0 & \cos\theta_y \end{bmatrix} \begin{bmatrix} -d/2 \\ 0 \\ 0 \end{bmatrix}. \tag{7} $$

where d is the distance between two virtual tip positions which is calculated to assign virtual dynamics (spring constant: s_v) to the virtual object as follows:

$$ F_g^r = s_v \frac{1}{d}, \quad d = \Delta\theta_p = \left| {}^{V}q_i - {}^{V}q_j \right|. \tag{8} $$

Then, each slave's tip position based on the virtual object is:

$$ {}^{V}q_i = {}^{V}q_m + {}^{V}q_{mi}, \quad {}^{V}q_j = {}^{V}q_m + {}^{V}q_{mj}. \tag{9} $$

4.3 Force feedback strategy

Here the question "what kind of haptic feedback is efficient?" arises. To answer this question, we need to consider the several factors including the contact type between the end-effector tip and the object. A haptic feedback contributes to increase the operability of human resulting in the improved overall performance of manipulation. Considering that our concern is to develop the single-master multi-slave telemicromanipulation framework, the conventional master, slave direct force feedback is not feasible. As shown in the Figure.4.8, in the case of 1:1 master slave system, a direct feedback from the force sensor is an effective for recognizing the slave side by human. If an 1:N master slave system as the grasping an object by human's hand with five fingertips, still human recognizes the grasping condition from multiple fingertip sensing. To assure the stable grasping in 1:N

system, each end-effector of N slave devices should cooperate with each other to regulate the grasping force by transferring the grasping force to the human operator through the haptic interface. This strategy helps to regulate the grasping force by both the human's control and robot's control. Looking it in coordinate system, the exerted force by the object to the slave and the feedback forces in case of 1:1 feedback strategy are denoted as ${}^{R}f_i$ and ${}^{U}f_i$ respectively. These are scaled between the master and the slave to amplify the force in the micro environment. However, in the case of 1:N feedback strategy, it is assumed that the virtual thread exerting the feedback force (${}^{U}f_i$) to the human operator by the slave's applied forces (${}^{R}f_i$) to the object.

Then, the force diagram between the multi-slaves and the object should be analyzed to calculate the proper feedback to the user.

μ denotes the friction coefficient between the object and the slave. f_i is the internal force term at the i^{th} slave's contact position. μf_i describes the frictional force upward caused by the internal force (f_i at a i^{th} contact position. θ_r denotes the commanded roll angle of the manipulated object which forms the orthogonal downward force ($\mu f_i \cos\theta_r$). If N slaves are handling an object, the resisting force (F) downward is,

$$F = \mu N f_i \cos\theta_r \tag{10}$$

Assuming that the scaling factor between the master and the slave for micromanipulation tasks is given as,

$$A_p = diag(A_p, A_p, A_p) \tag{11}$$

Then the feedback force to the human operator which is defined here as the ${}^{U}f_i$ is obtained from,

$${}^{U}f_i = A_p F \tag{12}$$

A question is now arising mainly about how to obtain f_i in real time and deliver it to user. The simple calculation to obtain f_i is implemented to the SMMS system in section 4.4.

4.4 Internal force decomposition

When multiple manipulators grasp an object, the force applied by multiple robots can be decomposed into motion-inducing force and internal force. Especially, the internal force should be kept in a certain range to assure the stable grasping and safety of object. In the proposed cooperative master–slave manipulation system, the internal force to squeeze the grasped object is fed into the human operator through the master haptic device. Figure 5 depicts two manipulators cooperating to grasp a single object.

Force decomposition using the theory of metric spaces and generalized inverses was attempted (Bonitz & Hsia, 1994). It is assumed that each manipulator grasps the object rigidly, exerting both forces and moments on the object. The net force at the object frame is related to the forces applied by the manipulators by:

$$f_{obj} = J_o^T f \tag{13}$$

where $f_{obj} = \begin{bmatrix} f_o^T & m_o^T \end{bmatrix}^T$ is the net force and moment at the object frame, $J_o^T = \begin{bmatrix} J_{o1}^T & J_{o2}^T \end{bmatrix}$. J_{oi} is the Jacobian from the object frame to the i^{th} end-effector frame, $f = \begin{bmatrix} f_1^T & m_1^T & f_2^T & m_2^T \end{bmatrix}^T$. f_i is the force and m_i is the moment applied by the i^{th} end-effector. $p_i = \begin{bmatrix} p_{ix} & p_{iy} & p_{iz} \end{bmatrix}^T$ is the vector from the i^{th} end-effector to the object frame:

$$J_{oi}^T = \begin{bmatrix} I_3 & O_3 \\ -P_i & I_3 \end{bmatrix}^T \tag{14}$$

$$P_i = \begin{bmatrix} 0 & -p_{iz} & p_{iy} \\ p_{iz} & 0 & -p_{ix} \\ -p_{iy} & p_{ix} & 0 \end{bmatrix} \tag{15}$$

The applied force f is decomposed into motion-inducing, f_M, and internal, f_I, with:

$$f_I = (1 - J_o^{T\Phi} J_o^T) f, \tag{16}$$

Where, $J_o^{T\Phi} J_o^T$ is a generalized inverse of J_o^T. The projections $P_M = J_o^{T\Phi} J_o^T$ and $P_I = I - J_o^{T\Phi} J_o^T$ project the applied force onto the motion inducing force subspace, F_M, and the internal force inducing force subspace, F_I, respectively. If $rank(J_o^T M J_o) = rank(J_o^T)$, the weighting matrix M can be used to compute a generalized inverse of J_o^T. Therefore:

$$J_o^{T\Phi} = M J_o (J_o^T M J_o)^{-1} = \frac{1}{2} \begin{bmatrix} I_3 & O_3 \\ P_1 & I_3 \\ I_3 & O_3 \\ P_2 & I_3 \end{bmatrix}. \tag{17}$$

Using (13) and (14), the decomposition of f is:

$$f_I = \begin{bmatrix} f_1 - f_2 \\ m_1 + (P_2 - P_1) f_2 - m_2 \\ -(f_1 - f_2) \\ (P_1 - P_2) f_1 - m_1 + m_2 \end{bmatrix}. \tag{18}$$

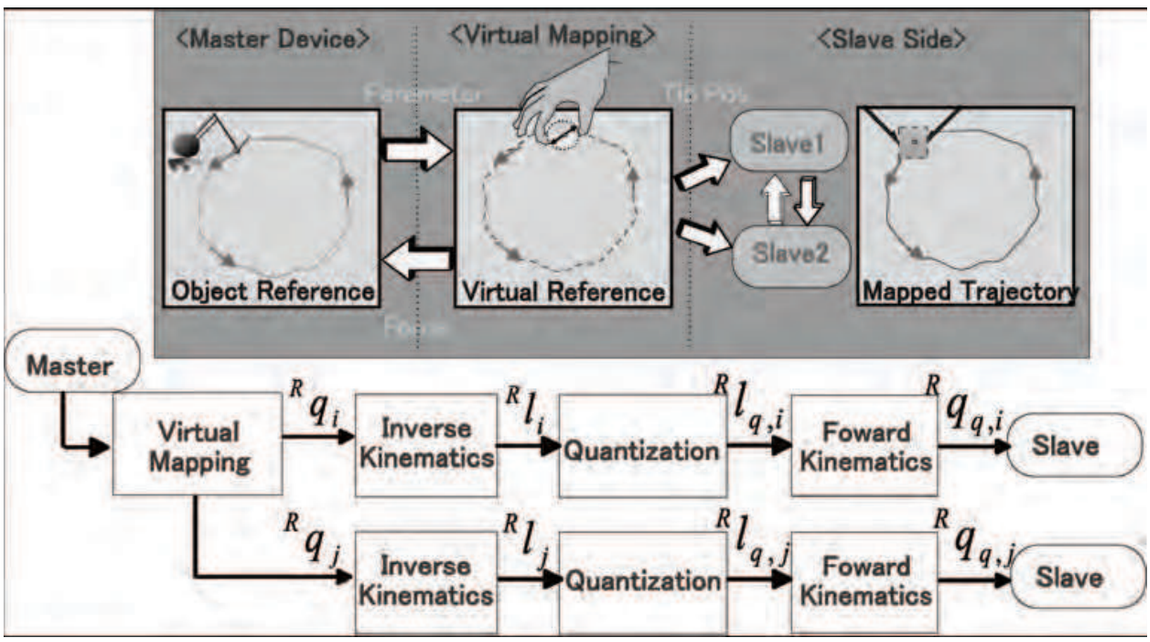

Fig. 6. Virtual mapping experiment: ${}^{R}q_{i,j}$ are robot's Cartesian references, ${}^{R}l_{i,j}$ are robot's link coordinates, ${}^{R}l_{q,i}$ and ${}^{R}l_{q,j}$ are quantized robot link configuration and ${}^{R}q_{q,i}$ and ${}^{R}q_{q,j}$ are resultant robot control configuration.

4.5 Manipulation strategy

In much previous master–slave manipulation research, the whole task was done by only the human operator.

However, in the case of the SMMS system, there exist d.o.f. differences between the master and the slave. Therefore, it is a good idea to build a whole manipulation process with several task phases.

In this paper, a human machine cooperative manipulation strategy is proposed as shown in Fig. 6. User is assumed to monitor the target object under the two-dimensional (2-D) visual information on the task space.

As a first phase, both slave manipulators approach to the target object following the reference position scaled from the haptic device operated by the human. Once one of both end-effectors is contacted with object, the grasping phase is started. An autonomous grasping algorithm leads to a stable grasp. Then, the user makes a movement of the target object grasped between both end-effectors. To release the object, operator needs to lead the object to be touched on the ground. The problem caused by the d.o.f. difference between the master and the slave is overcome through the proposed manipulation strategy.

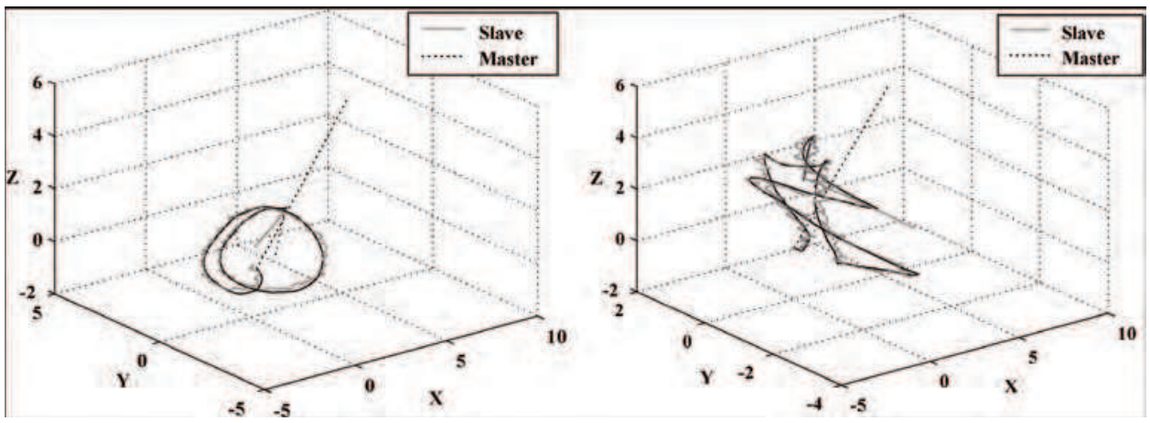

(a) (b)

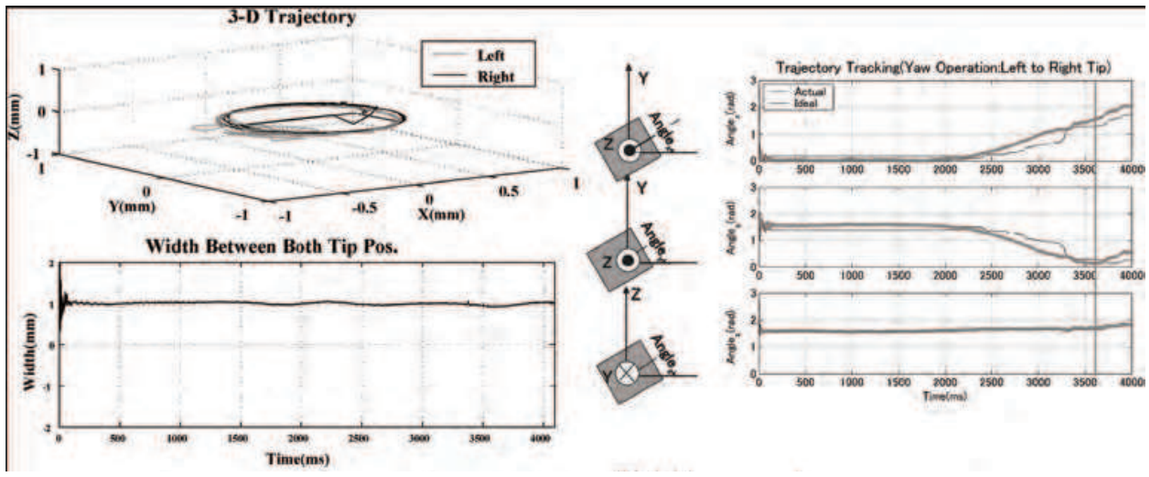

(c) (d)

Fig. 7. Dual-micromanipulator's manipulability (w). Upper and lower panels show the left and right manipulators, respectively.

5. Experiments

5.1 Positioning accuracy experiment

First of all, a rectilinear movement experiment was performed to evaluate the system's overall positioning accuracy, which is a trade-off with manipulability. Figure 6 shows the parallel line drawing. Intervals between lines of 10 μm were used. Observed intervals of parallel lines are about 11 μm. In this case intervals are not the same as the reference intervals; however, almost regular intervals were observed. Movement error is caused by an encoder resolution which was set as 0.122 μm.

5.2 Trajectory tracking experiment

Figure 6 describes the controller of an overall system to show the mapping. An experiment on micro-positional synchronization using our micromanipulation system was conducted.

The user operates the PHANToM device with a 3-D random or circular trajectory. This PHANToM reference trajectory generated by the human operator contains the scale factor between the master and the slave. The trajectory of the PHANToM reference and the resulting trajectory of both end-effectors centre position is shown in Fig. 7a,b. We generated two different trajectories which are circular and random motions with a single master device. The following trajectory of both slave end-effectors centre position is depicted as a solid line. The validity of our proposed positional mapping method in real-time operation is verified with this result. Through the result shown in Fig. 7a,b, both slave end-effectors are kept at a certain width during the experiment. The reference trajectory of the single master device is controlling two slave devices without coupling them to smaller scale applications such as micro- and nanomanipulations, which require higher positioning accuracy. These results strengthen the feasibility of the single-master controlled multi-slave system.
Other experiments were conducted to verify the proposed object mapping method. A human operator is handling a 1 cm^3 cubic object with the PHANToM haptic interface. In Fig. 5, the vector from the left to right contact position is defined as:

$$ {}^{R}q_{12} = {}^{R}q_{2} - {}^{R}q_{1}, \tag{17} $$

Where ${}^{R}q_{i}$ depicts the i^{th} contact position in the robot coordinate system. The yaw angle of the virtual object is controlled by a sinusoidal wave or the human operator's arbitrary operation. First, the sinusoidal yaw angle input is given to prove the proposed mapping method. Figure 7c,d show the 3-D trajectory of both end-effectors' tip positions and the width between them. The reference position of the virtual centre is constrained to be static. It is verified that the width is kept static during the operation. The reference roll, pitch and yaw angles are converted between the user's frame and the robot's frame as follows:

$$ {}^{R}\theta_{y,ref} = \frac{1}{36}\,{}^{U}\theta_{y,ref} + 1.0, \tag{18} $$

$$ {}^{R}\theta_{p,ref} = 0.05\,{}^{U}\theta_{p,ref}, \tag{19} $$

$$ {}^{R}\theta_{r,ref} = 0.1\,{}^{U}\theta_{r,ref}, \tag{20} $$

These reference inputs are decided empirically by considering both the workspace and object scale. The experimental results are shown here. In Fig. 7d, the object's orientation is shown following the yaw operation by the human operator. Anglex , Angley and Anglez are angles between ${}^{R}q_{12}$ and each axis. These results show that the developed SMMS system can realize low-cost, object based 6 d.o.f., and even compact-sized moment control by both slaves' translational movement. It is promising to the development of dexterous micro/nanomanipulation system with ultra-high precision positioning accuracy.

5.3 Force mapping experiment

Several experiments were further performed to verify how feasible it is for us to adopt the decomposed internal force derived in section 4. Another purpose of this experiment is to obtain the desired internal force for stable grasping during several primitive tasks. A square

stylen block 10 mm in width, length and height was used in this experiment. Figure 16 shows the internal force plotted for several grasping phases such as keeping the grasped object, parallel movement and 10 times iterative grasping/releasing. Transferring force to the user gives the teleoperation more transparency which is closely correlated to the user operability and the task performance. In the case of used stylen bock experiment, it is found that a reasonable choice of the internal force during the grasp phase should be made around 5 mN in each direction. Also, the Figure 6 describes the controller of a phase transition should be done by the event which is the change of internal force around the transition phase. Especially, in the iterative grasping/releasing phase, it is possibly able to be used for compensating the deficiency of the master's d.o.f.

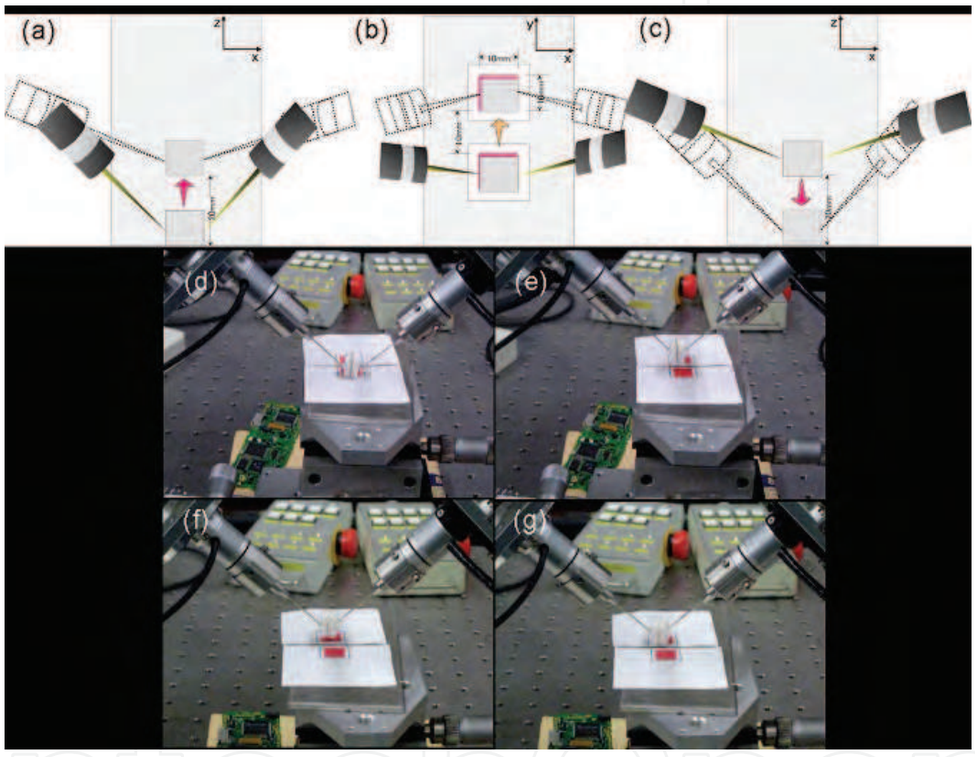

Fig. 8. Styren block pick-and-place experiment: schematic (a) pick up 10 mm (b) move 10 mm (c) release onto substrate. Operation: (d) grasp (e) pick up (f) move (g) release.

5.4 Pick-and-place of styrene block

We conducted several experiments using a 10 mm cubic styrene block, roe (4-6 mm) to demonstrate the feasibility of our proposed system for deformable objects in different scale and mechanical properties.

First, pick-and-place of a stylen cubic block (1 cm^3) was performed to show validity of the proposed dexterous manipulation strategy. Figure 8 shows the demo experiment. The distance between the initial and the target point is 1 cm. The human operator recognizes the target object from the visual display of the microscope and operates the single haptic interface to the contact position of the object. Then, the pitch angle of the haptic interface is controlled by the user to give enough grasp force with the internal grasp force display.

Then, the grasped object is moved to the target goal. To release the grasped object, the pitch angle is controlled again by the user with the feeling of internal force.
Force sensors at each end-effector measure real-time 6 axial force data and implement low-level internal grasping force to the user through the haptic interface and network between the master and slave (Fig. 9). The user`s work speed is recorded to clearly define mode transition time. Styrene block handling assumes stable contact between the probe and styrene block, which causes higher friction at the probe that could damage membranes in real cell handling. But it is sufficient to show the feasibility of our proposal in biotweezing even as small as on the smaller scale. It also demonstrates amplified motion without being limited by microscope depth-of-focus problems during pick-and-place tasks.

5.5 Salmon roe pick-and-place

After confirming feasibility in preliminary experiments, we conducted cell handling and injection using roe from 4 to 6 mm in diameter, which is easy to obtain and provides visual feedback without the need for a microscope (Fig. 10). To handle smaller cells, it is necessary to solve autofocusing problems.

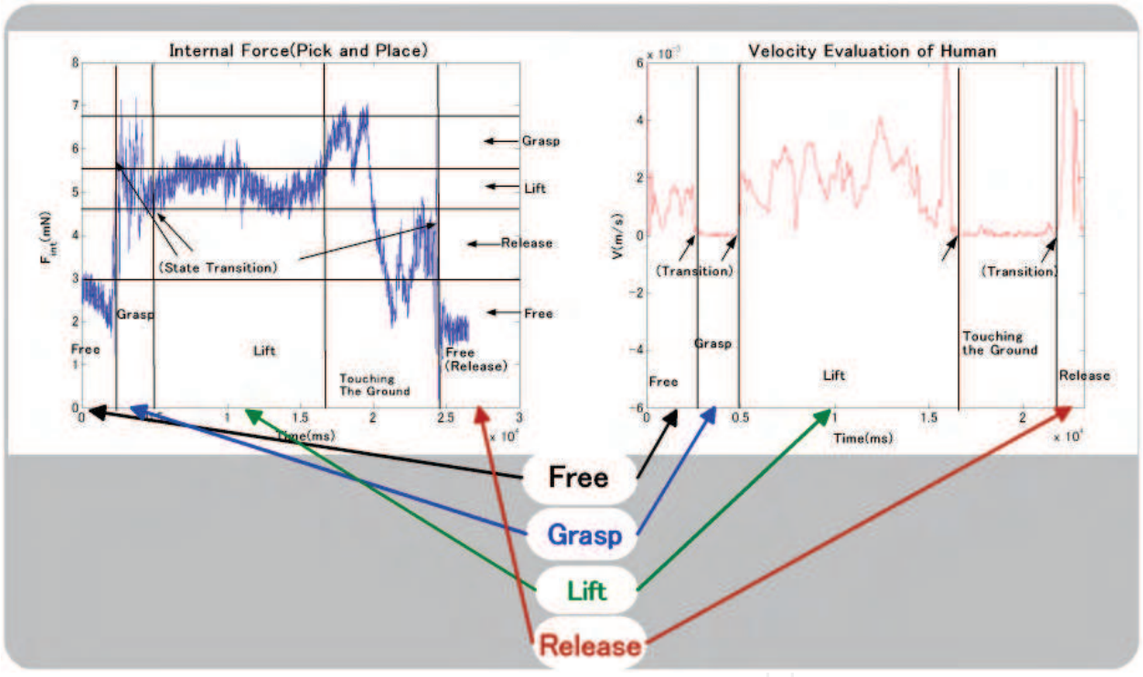

Fig. 9. Internal force during the styrene block pick-and-place operation and user operation speed evaluation.

6. Conclusion & outlook

We have shown a dexterous micromanipulation system based on single-master and multi-slave device configuration and its deformable object micromanipulation such as styrene block and roe. The system enables 6 d.o.f. object position control using 2 parallel mechanism micromanipulators. It has potential applications for manipulating, characterization, complicated device assembly, and biological cell manipulation. In addition to the

manipulation dexterity, an object based 6 d.o.f. control was achieved using compact size low-cost moment control which has enough accuracy by using multiple slaves translation motion. First, we analyzed parallel mechanism and multiple manipulators kinematics and further evaluated the singular position and manipulability of the system. Second, one of the most serious problems, i.e., such as the mapping method between the master and the slave, was discussed. A novel micromanipulation strategy which is the most feasible for the SMMS system was given. Experimental results including styrene block and salmon roe manipulation were shown to verify the feasibility of the proposed method to wide variety of applications. In parallel, we have already developed a human–robot shared internal grasp force control via a network using a SMMS system. The stability analysis on the controller passivity over delayed communication is being performed. Also, virtual fixture-based haptic guidance tele-micromanipulation to improve human operability is implemented on the SMMS system and evaluated from the viewpoint of human operability and task performance, which can be challenging research. Finally the proposed system will further be implemented in smaller scale manipulations by improving the conventional sensing and actuation limitation.

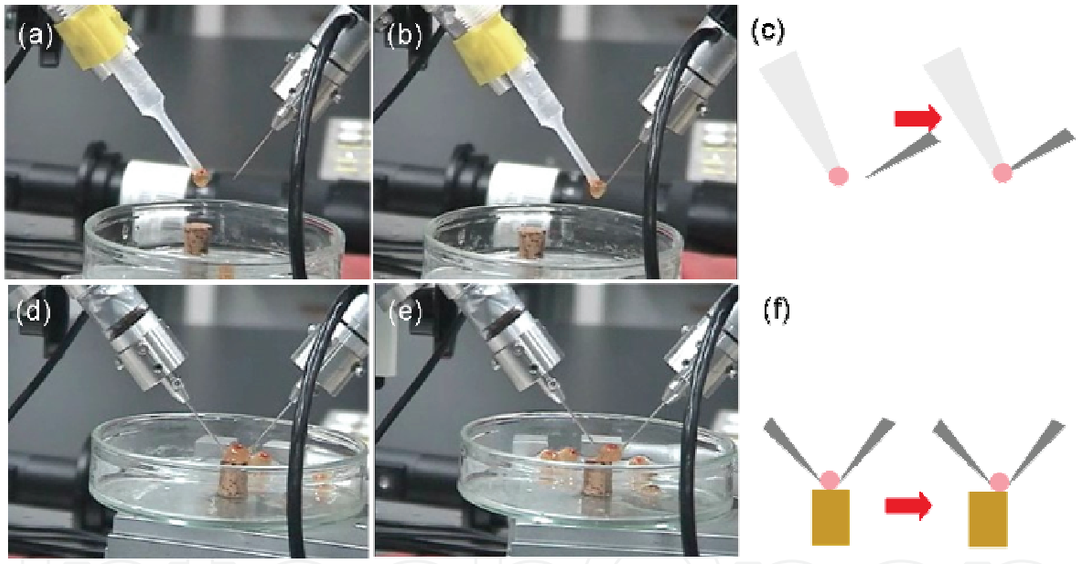

Fig. 10. Screenshots of salmon roe tweezing, indentation (a,b,c) and pick-and-place experiment (d,e,f).

7. References

Ando, N.; Korondi, P & Hashimoto, H. (2001). Development of micromanipulator and haptic interface for networked micromanipulation, *IEEE/ASME Transactions on Mechatronics*, Vol.6, No.4, pp.417–427, ISSN 1083-4435.

Ando, N.; Suehiro, T.; Kitagaki, K.; Kotoku, T. & Yoon, W. (2005). Implementation of RT composit components and a component manager, *Proceedings of the 2005 IEEE/RSJ International Conference on Intelligent Robots and Systems*, Vol.1, pp.3933–3938, ISBN 0-7803-8912-3, Edmonton, Canada, Aug. 2005.

Bonitz. R. & Hsia, T. (1994). Force decomposition in cooperating manipulators using theory of metric spaces and generalized inverses, *Proceedings of 1994 IEEE International*

Conference on Robotics and Automation, Vol.2, pp.1521–1527, ISBN 0-8186-5330-2, San Diego, USA, May. 1994.

Cleary, K. & Arai, T. (1991). A prototype parallel manipulator: kinematics, construction, software, workspace results, and singularity analysis, *Proceedings of the 1991 IEEE International Conference on Robotics and Automation*, Vol.1, pp.566–57, ISBN 0-8186-2163-X, Sacramento, USA, Apr. 1991.

Dosis, A.; Bello, F.; Rockall, T.; Munz, Y.; Moorthy, K.; Martin, S. & Darzi, A. (2003). ROVIMAS: a software package for assessing surgical skills using the da Vinci telemanipulator system, *Proceedings of 4th International IEEE EMBS Special Topic Conference on Information Technology Applications in Biomedicine*, Vol.1, pp. 326-329, ISBN 0-7803-7667-6, Birmingham, UK, Apr. 2003.

Fichter, E. F. (1986). A Stewart-Platform based manipulator: general theory and practical construction, *International Journal of Robotics Research*, Vol.5, No.2, pp.157–182, ISSN 0278-3649.

Griffin, W. B.; Provancher W. R. & Cutkosky, M. R. (2003). Feedback strategies for shared control in dexterous telemanipulation, *Proceedings of the 2003 IEEE/RSJ International Conference on Intelligent Robots and Systems*, Vol.3, pp.2791–2796, ISBN 0-7803-7860-1, Las Vegas, USA, Oct. 2003.

Hannoford, B. & Anderson, R. (1988). Experimental and simulation studies of hard contact in force reflecting teleoperation, *Proceedings of the 1995 IEEE International Conference on Robotics and Automation*, Vol.1, pp.584–589, ISBN 0-8186-0852-8, Pittsburgh, USA, Apr. 1988.

Hwang, G. & Hashimoto, H. (2007). Development of a single-master multi-slave tele-micromanipulation system, *Advanced Robotics*, Vol.21, No.3-4, pp.329–349, ISSN 0169-1864.

Kosuge, K.; Ishikawa, J.; Furuta, K. & Sakai, M. (1990). Control of single-master multi-slave manipulator system using VIM, *Proceedings of the 1990 IEEE International Conference on Robotics and Automation* , Vol.1, pp.1172–1177, ISBN 0-8186-9061-5, Cincinnati, USA, May. 1990.

Kosuge, K.; Itoh T.; Fukuda T. & Otsuka, M. (1995).Tele-manipulation system based on task-oriented virtual tool, *Proceedings of the 1995 IEEE International Conference on Robotics and Automation*, Vol.1, pp.351–356, ISBN 0-7803-1965-6, Nagoya, Japan, May. 1995.

Lee D. J. & Spong, M. W. (2005). Bilateral teleoperation of multiple cooperative robots over delayed communication networks: theory, *Proceedings of 2005 IEEE International Conference on Robotics and Automation*, Vol.1, pp.360-365, ISBN 0-7803-8914-X, Barcelona, Spain, Apr. 2005.

Paul, R. P. (1981). *Robot Manipulators: Mathematics, Programming, and Control*, ISBN 0-2621-6082X, MIT Press, Cambridge, USA.

Tanikawa, T. & Arai, T. (1999). Development of a micro-manipulation system having a two-fingered micro-hand, *IEEE Transactions on Robotics and Automation*, Vol.15, No.1, pp.152–162, ISSN 1042-296X.

Thompson J. A. & Fearing, R. S. (2001). Automating microassembly with ortho-tweezers and force sensing, *Proceedings of the 2001 IEEE/RSJ International Conference on Intelligent Robots and Systems*, Vol.1, pp.1327–1334, ISBN 0-7803-6612-3, Hawaii, USA, Nov. 2001.

Yoshikawa, T. (1985). Manipulability of robotic mechanisms, *International Journal of Robotics Research*, Vol.4, No.2, pp.3–9, ISSN 0278-3649.

Parallel Manipulators, New Developments

Edited by Jee-Hwan Ryu

ISBN 978-3-902613-20-2

Hard cover, 498 pages

Publisher I-Tech Education and Publishing

Published online 01, April, 2008

Published in print edition April, 2008

Parallel manipulators are characterized as having closed-loop kinematic chains. Compared to serial manipulators, which have open-ended structure, parallel manipulators have many advantages in terms of accuracy, rigidity and ability to manipulate heavy loads. Therefore, they have been getting many attentions in astronomy to flight simulators and especially in machine-tool industries.The aim of this book is to provide an overview of the state-of-art, to present new ideas, original results and practical experiences in parallel manipulators. This book mainly introduces advanced kinematic and dynamic analysis methods and cutting edge control technologies for parallel manipulators. Even though this book only contains several samples of research activities on parallel manipulators, I believe this book can give an idea to the reader about what has been done in the field recently, and what kind of open problems are in this area.

InTech Europe
University Campus STeP Ri
Slavka Krautzeka 83/A
51000 Rijeka, Croatia
Phone: +385 (51) 770 447
Fax: +385 (51) 686 166
www.intechopen.com

InTech China
Unit 405, Office Block, Hotel Equatorial Shanghai
No.65, Yan An Road (West), Shanghai, 200040, China
中国上海市延安西路65号上海国际贵都大饭店办公楼405单元
Phone: +86-21-62489820
Fax: +86-21-62489821

IntechOpen